www.czasopisma.pan.pl PAN POLSKA AKADEMIA NAUK www.journals.pan.pl

Arch. Metall. Mater. **62** (2017), 2B, 1383-1387

DOI: 10.1515/amm-2017-0213

D.-J. KIM*#, K.M. KIM*, J.H. SHIN*, Y.M. CHEONG*, E.H. LEE*, G.G. LEE*,
S.W. KIM*, H.P. KIM*, M.J. CHOI*, Y.S. LIM* AND S.S. HWANG *

OXIDATION BEHAVIOR OF STEEL WITH Cr CONTENT AND WATER FLOW RATE

Fast water flow facilitates ferrous ion transport leading to flow accelerated corrosion (FAC) of carbon steel and the possibility of a large accident through a failure of a secondary pipe in a nuclear power plant. Ion transport is directly linked to oxide properties such as the thickness, chemical composition and porosity. This work deals with a precise observation of the cross section of the corroded specimen focusing on an oxide passivity and its thickness using SEM (scanning electron microscope) and TEM (transmission electron microscope) as well as an apparent weight loss and a surface observation for the specimens corroded using a rotating cylindrical electrode autoclave system in pure water of pH 7 at 150°C having dissolved oxygen below 1 ppb within a flow rate range of 0 to 10 m/s. The Cr content in steel was changed from 0.02 to 2.4 wt%. Increasing the Cr content in the alloy, the FAC rate and oxide thickness decreased. The oxide porosity tends to decrease with the Cr content and immersion time owing to the development of Cr containing oxide. The oxidation behavior is not changed with the immersion time.

Keywords: Steel, flow accelerated corrosion, Cr content, flow rate, surface oxide

1. Introduction

Thousands of pipes made of carbon steel are exposed to high temperature, high pressure, and fast flowing water in a nuclear power plant. Ferrous ion tends to dissolve on the steel surface up to equilibrium solubility and transports to bulk water during the operation. A fast water flow facilitates ferrous ion transport leading to flow accelerated corrosion (FAC). FAC can lead to a large accident through a failure of a secondary pipe in a nuclear power plant [1]. Oxide formed on a steel surface can act as a barrier for ferrous ion transport.

Because ion transport is directly linked to the oxide property such as the thickness, chemical composition and porosity, there are numerous studies on the oxidation behavior in an exposed environment [2-6]. Fig. 1 describes the FAC occurring in steel alloy exposed to a flowing solution schematically.

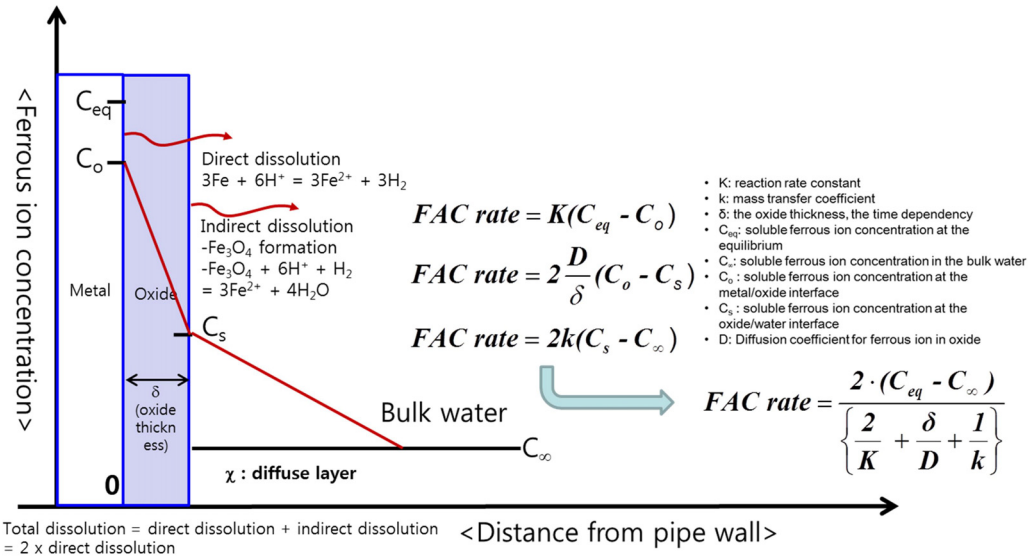

Fig. 1. Schematic diagram of ferrous ion concentration vs. distance from a pipe wall during FAC

* NUCLEAR MATERIALS SAFETY RESEARCH DIVISION, KOREA ATOMIC ENERGY RESEARCH INSTITUTE, DAEDEOK DAERO 989-111, YUSEONG, DAEJEON, KOREA, 34057

Corresponding author: djink@kaeri.re.kr

When oxide is passive, C_o, D and C_s decrease, the concentration gradient in a diffuse layer ($\Delta C/x$) decreases, and hence the FAC rate decreases. In the case of porous oxide, C_o, D and C_s increase, causing an increase in the concentration gradient in a diffuse layer ($\Delta C/x$), and the FAC rate to increase. When increasing the flow rate, the diffuse layer length (x) decreases and the concentration gradient increases in a diffuse layer ($\Delta C/x$), leading to an increase in the FAC rate.

The FAC rate can be formulated in three forms, as shown in Fig. 1, assuming that the total dissolution rate of ferrous ions is composed of a direct dissolution and indirect dissolution, the rates of which are the same [7]. From the FAC rate formulation, it is presumed that the oxide thickness and diffusion coefficient related to oxide porosity is closely related to the FAC phenomena. However, there have been few reports on an oxide investigation based on a TEM analysis, as a function of the Cr content and flow rate, which are key parameters affecting the FAC.

This work deals with a precise observation of the cross section of the corroded specimen focusing on an oxide passivity and thickness change using SEM (scanning electron microscope) and TEM (transmission electron microscope), as well as an apparent weight loss and a surface observation for the corroded specimens. Oxidation behaviors were investigated in view of the Cr content in the alloy and flow rate in a pure water of pH 7 at 150°C with dissolved oxygen below 1 ppb up to an elapsed time of 4000 h.

2. Experimental

The chemical compositions of materials used in this work are shown in Table 1. The Cr content in the alloy was ranged from 0.02 to 2.4wt%. The specimen geometry was 30 mm long, 20 mm wide, and 3 mm thick. Specimens were cleaned in water, degreased in acetone with an ultrasonic and then dried. The initial weights of the specimens before the experiment were measured.

An FAC test was performed at 150°C and at a pH of 7 for inlet water and flow velocities which were estimated from the angular velocities of a rotating cylinder of 0, 2, 4 and 10 m/s using a rotating cylindrical specimen, shown in Fig. 2. The test solution is circulated to control the pH and remove the dissolved ionic species with a flow rate of 50 cc/min through a test loop equipped with an ion exchanger.

After a high-temperature experiment, the weight of the specimen was measured following ultrasonic cleaning to estimate the corrosion rate and destructive observations using SEM (scanning electron microscope) and TEM (transmission electron microscope) were performed. The TEM sample used to examine the oxide cross section was prepared using an FIB (focused ion beam).

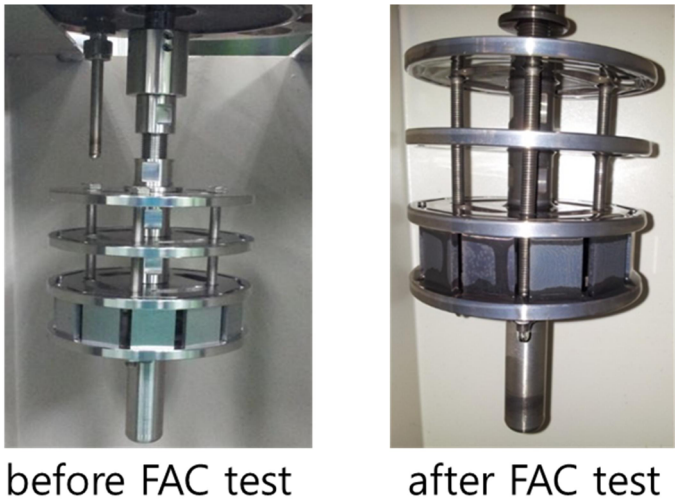

Fig. 2. Rotating cylindrical specimen and holder attached to autoclave for FAC test

3. Results and discussion

Fig. 3 shows (a) the FAC rate and (b) an SEM image of a cross section for various materials after 3170 exposure. The FAC rate was obviously decreased with the Cr content in the alloy. The oxide thickness and roughness were also decreased with the Cr content in the order of SA106, SA487, and A534. Fig. 4 also shows the TEM image of the cross section for various materials after 3170 exposure. In addition to the oxide thickness and roughness based on an SEM image, which can cover a larger area than a TEM image, it is noted that the oxide porosity was decreased with the Cr content in the alloy. This indicates that the Cr in the alloy affects the oxide property such as the thickness, roughness and porosity, leading to a decrease in the FAC rate.

Magnetite, Fe_3O_4 not containing Cr, which forms on carbon steel under a high-temperature aqueous solution with a low dissolved oxygen is not protective, allowing a continuous dissolution of ferrous ion and hence a high FAC rate and oxide thickness. The local roughness is also increased, caused by active FAC as shown in Fig. 3b. However, when the Cr content is increased in the alloy, Cr is incorporated into the oxide, enhancing the oxide passivity and decreasing the FAC rate and roughness. It is

TABLE 1

Chemical composition of specimens

Material	Cr	Mo	V	Cu	Mn	Ni	Si	Ti	C	P	S
A106 Gr.B	0.02	0.01		0.04	0.37	0.02	0.22		0.19	0.008	0.006
A508 Gr.3	0.17	0.46	0.001	0.03	1.22	0.68	0.21	0.002	0.22	0.007	0.002
A534 8620H	0.47	0.15~0.30		Max 0.3	0.6~0.9	0.4~0.7	0.15~0.35		0.17~0.23	Max 0.03	Max 0.03
A508 Gr.4N	1.80	0.49	0.003	0.001	0.33	3.44	0.21	0.006	0.18	0.0029	0.0019
A336 F22V	2.40	0.9	0.25	0.1	0.4	0.1	0.1	0.01	0.10	0.006	0.001

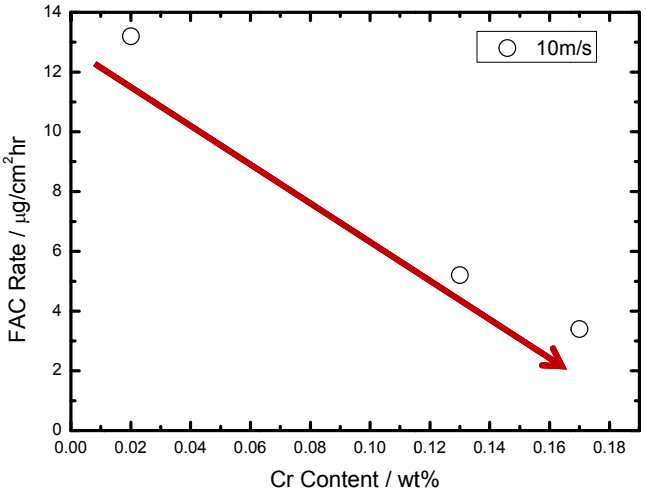

(a)

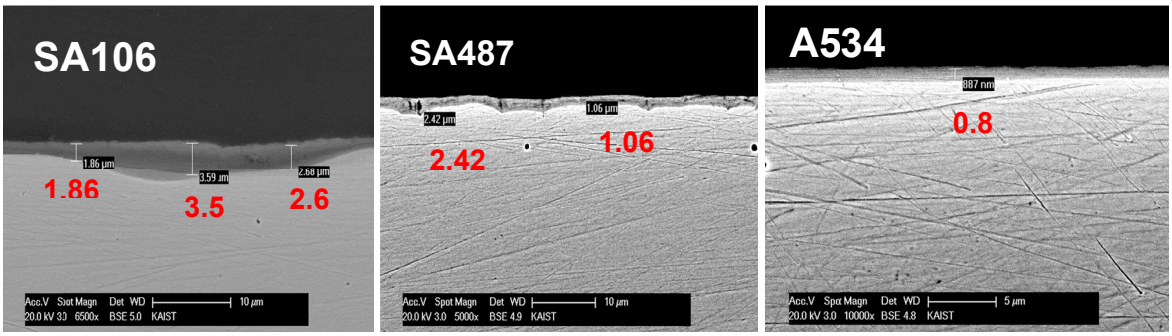

(b)

Fig. 3. (a) FAC rate and (b) SEM images of cross section for various materials after 3170 exposure

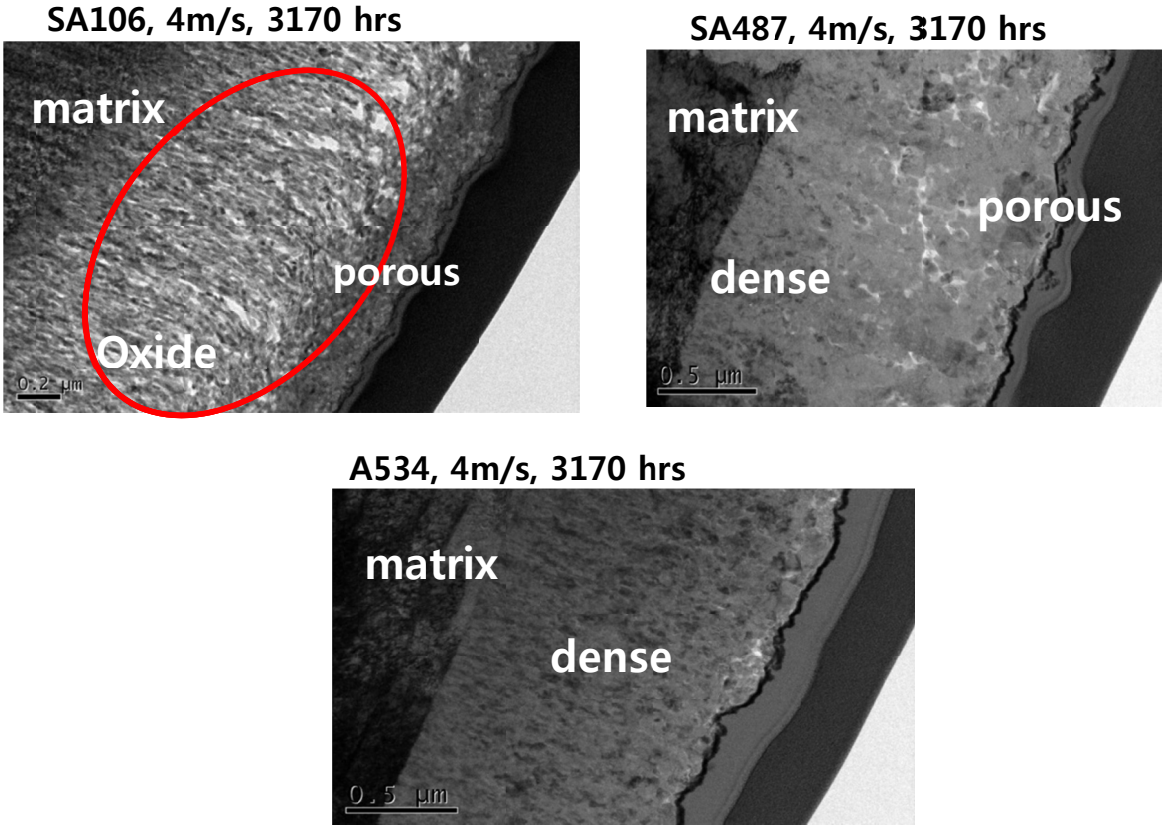

Fig. 4. TEM images of cross section for various materials after 3170 exposure

known [2,3] that Cr oxide is more passive than Fe oxide, and its application as corrosion resistant treatment such as stainless steel is widely used. It was also reported [8] that the Cr is enriched in the oxide over time because the Cr solubility is lower than that of the Fe in the solution.

Table 2 shows the relative oxide porosity defined as the ratio of corrosion rate (= corrosion rate of interesting alloy / corrosion rate of carbon steel (SA106)), assuming that the oxide formed on carbon steel (SA106) is perfectly porous. Similarly, the relative oxide passivity can be defined as relative oxide porosity subtracted from unity.

$$\textit{Relative oxide porosity} = \frac{\textit{corrosion rate of an alloy}}{\textit{corrosion rate of SA106}} \quad (1)$$

From Table 2, SA508 containing Cr of 0.17wt% shows a better passivity than SA487 containing Cr of 0.13wt%. The oxide passivity was improved with the exposure time, which may be attributed to an enrichment of Cr in the oxide. The Cr can be enriched on surface with the immersion time due to solubility difference between Fe and Cr leaving more passive oxide on the surface.

TABLE 2

Relative oxide porosity for SA487 and SA508 as a function of the exposure time

Exposure time (hr)	840	1670	2510	2930	Remark
SA487	0.3	0.2	0.2	0.2	Time dependency
SA508	0.2	0.1	0.1	0.1	Better passivity

Fig. 5 shows the FAC rate with the flow rate for SA106. When the flow rate increases, the diffuse layer length is decreased, leading to a concentration gradient increase in the diffuse length and thus an FAC rate increase. It was reported [9] that the diffuse layer length is decreased from 0.5 to 0.01 mm when solution is stirred.

Fig. 6 shows the surface appearance with a flow rate for SA106 after 1670 h of exposure. A pit like morphology was seen and developed with a flow rate in view of the number of pits. It was shown that a pit like morphology is caused by the inclusion dissolution at the early stage, and is developed into

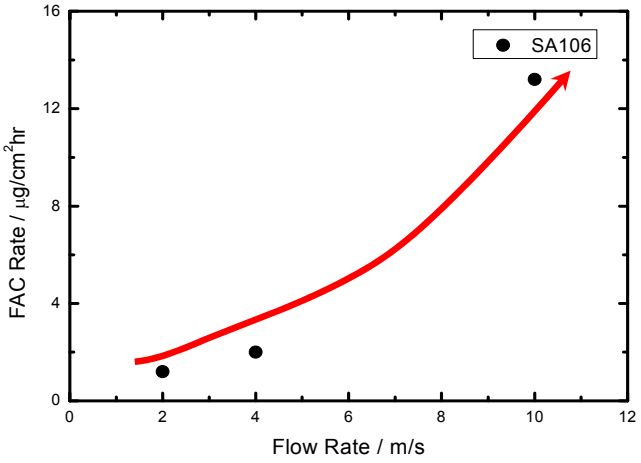

Fig. 5. FAC rate as a function of the flow rate for SA106

a scallop (orange peel) pattern [10]. From this, it is presumed that the density and size of a pit like morphology is an index of the FAC rate.

Fig. 7 shows a TEM image of the cross section of SA106 after 1670 h of exposure. The oxide thickness was decreased with the flow rate. It seems that the oxide porosity is not changed with the flow rate, as shown in a TEM image. The FAC rate is increased and the oxide thickness is decreased, which is caused by the relative ease of the mass transfer at a relatively higher flow rate, while the FAC rate and oxide thickness are decreased with the Cr content in the alloy.

Table 3 shows the corrosion rate ratio defined as the ratio of corrosion rate (= corrosion rate at low flow rate / corrosion rate at high flow rate (10 m/s) for SA106) with the exposure time.

$$\textit{Corrosion rate ratio (flow rate)} = \frac{\textit{corrosion rate at low flow rate}}{\textit{corrosion rate at high flow rate}} \quad (2)$$

From Table 3, the corrosion rate ratio is not sensitive to the elapsed time of this work indicating that the corrosion kinetics is not changed with the time. From the results of Fig. 7 and Table 3, it seems that the FAC rate with the flow rate does not depend on the oxide formation kinetics but depends only on the mass transfer. Consequently, this leads to an insensitivity of oxide porosity with the flow rate, as shown in Fig. 7.

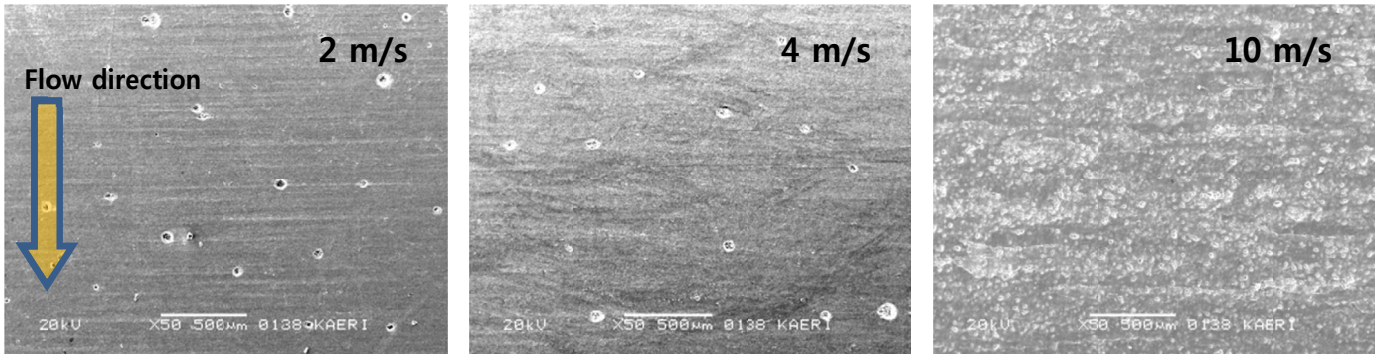

Fig. 6. Surface appearance with the flow rate for SA106 after 1670 h of exposure

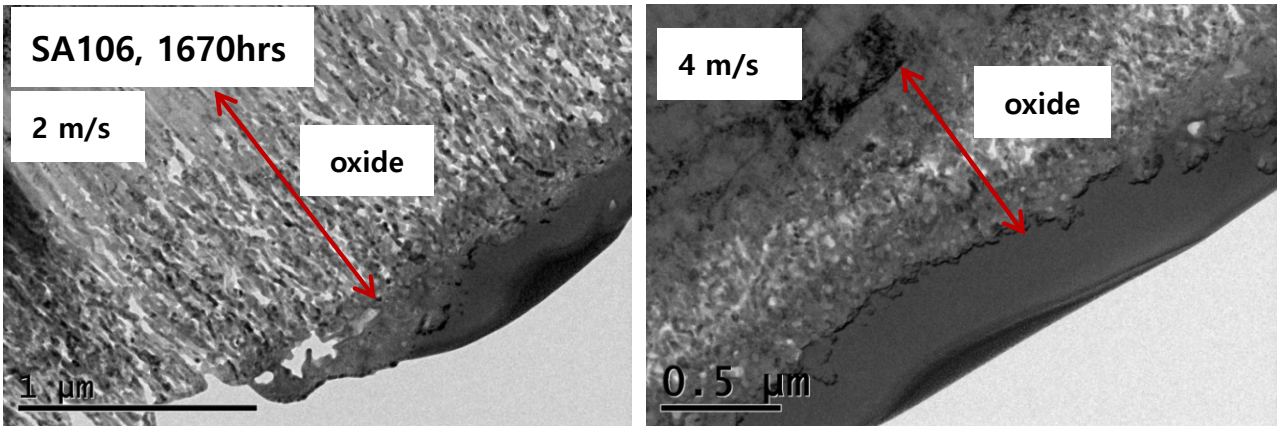

Fig. 7. TEM image of cross section for SA106 after 1670 h of exposure

TABLE 3

Corrosion rate ratio for SA106 as a function of the exposure time

Elapsed time (hrs)	410	1670	2090	2930	Remark
4 m/s	0.15	0.15	0.15	0.14	Insensitive to immersion time
2 m/s	0.11	0.09	0.09	0.08	

4. Conclusions

1. The FAC rate, oxide thickness and oxide porosity decreased with the Cr content in an alloy. The passivity is improved with the elapsed time owing to the development of Cr containing oxide.
2. The FAC rate was increased but the oxide thickness was decreased with the flow rate, while the oxide porosity is almost unchanged. The corrosion kinetics does not seem to be changed with the elapsed time. The pit density was increased with the flow rate based on the surface appearance.

Acknowledgments

This work was financially supported by the Ministry of Science, ICT and Future Planning (MSIP) of Korea.

REFERENCES

[1] Flow accelerated corrosion in power plants, EPRI report, TR--106611-R1, Palo Alto, CA, 1998.
[2] J. Robertson, Corrosion Science **29**, 1275 (1989).
[3] D.J. Kim, H.C. Kwon, H.P. Kim, Corrosion Science **50**, 1221 (2008).
[4] D.J. Kim, H.C. Kwon, H.W. Kim, S.S. Hwang, H.P. Kim, Corrosion Science **53**, 1247 (2011).
[5] S.Y. Kang, D.W. Lee, J. Korean Power Metallurgy Institute, **21**, 260 (2014).
[6] J.-P. Lee, J.-H. Hong, D.-K. Park, I.-S. Ahn, J. Korean Power Metallurgy Institute, **22**, 52 (2015).
[7] L.E. Sanchez-Caldera, P. Griffith, E. Rabinowicz, J. Engineering for Gas Turbines and Power **110**, 180 (1988).
[8] H. Abe, T. Yano, Y. Watanabe, M. Nakashima, T. Tatsuki, presented at FAC 2016, May 24-27, 2016, Lille, France.
[9] S.I. Pyun, The Fundamentals of Corrosion of Metals and Their Application into Practice, Chungwoongak 2006.
[10] H.P. Kim, M.J. Kim, D.J. Kim, presented at 19th ICC, Nov. 2-6, 2014, Jeju, Korea.